

# **B-cell malignancies - A new knowledge hub on the latest research in therapeutic advances**

**EDUCATIONAL CONTENT AVAILABLE ON  
THE HUB:**




- **On-demand Webinars - earn CME credit**
  - **Infographics**
  - **Patient Case Studies**
  - **Curated Research Articles**
- ...and much more**

**VISIT KNOWLEDGE HUB TODAY**

This educational resource has been supported by Eli Lilly.

**WILEY**

# [<sup>18</sup>F]-FDG PET radiomic model as prognostic biomarker in diffuse large B-cell lymphoma

Laura Lavinia Travaini<sup>1</sup>  | Francesca Botta<sup>2</sup> | Enrico Derenzini<sup>3,4</sup>  |  
Giuliana Lo Presti<sup>5</sup> | Mahila Esmeralda Ferrari<sup>2</sup> | Lighea Simona Airò Farulla<sup>1,6</sup>  |  
Tommaso Radice<sup>3,4</sup> | Saveria Mazzara<sup>7</sup> | Corrado Tarella<sup>3,4</sup> | Stefano Pileri<sup>7</sup> |  
Sara Raimondi<sup>5</sup> | Francesco Ceci<sup>1,6</sup>

<sup>1</sup>Division of Nuclear Medicine, IEO European Institute of Oncology, IRCCS, Milan, Italy

<sup>2</sup>Medical Physics Unit, IEO European Institute of Oncology IRCCS, Milan, Italy

<sup>3</sup>Oncohematology Division, IEO European Institute of Oncology IRCCS, Milan, Italy

<sup>4</sup>Department of Health Sciences, University of Milan, Milan, Italy

<sup>5</sup>Department of Experimental Oncology, IEO European Institute of Oncology IRCCS, Milan, Italy

<sup>6</sup>Department of Oncology and Hematology, University of Milan, Milan, Italy

<sup>7</sup>Haemolymphopathology Division, IEO European Institute of Oncology IRCCS, Milan, Italy

## Correspondence

Enrico Derenzini, Director of the Division of Hematology, IEO European Institute of Oncology IRCCS, Via G. Ripamonti 435, Milan 20141, Italy.

Email: [enrico.derenzini@ieo.it](mailto:enrico.derenzini@ieo.it)

## Abstract

To evaluate the association between radiomic features (RFs) extracted from <sup>18</sup>F-FDG PET/CT (<sup>18</sup>F-FDG-PET) with progression-free survival (PFS) and overall survival (OS) in diffuse large-B-cell lymphoma (DLBCL) patients eligible to first-line chemotherapy. DLBCL patients who underwent <sup>18</sup>F-FDG-PET prior to first-line chemotherapy were retrospectively analyzed. RFs were extracted from the lesion showing the highest uptake. A radiomic score to predict PFS and OS was obtained by multivariable Elastic Net Cox model. Radiomic univariate model, clinical and combined clinical-radiomic multivariable models to predict PFS and OS were obtained. 112 patients were analyzed. Median follow-up was 34.7 months (Inter-Quartile Range (IQR) 11.3–66.3 months) for PFS and 41.1 (IQR 18.4–68.9) for OS. Radiomic score resulted associated with PFS and OS ( $p < 0.001$ ), outperforming conventional PET parameters. C-index (95% CI) for PFS prediction were 0.67 (0.58–0.76), 0.81 (0.75–0.88) and 0.84 (0.77–0.91) for clinical, radiomic and combined clinical-radiomic model, respectively. C-index for OS were 0.77 (0.66–0.89), 0.84 (0.76–0.91) and 0.90 (0.81–0.98). In the Kaplan-Meier analysis (low-IPI vs. high-IPI), the radiomic score was significant predictor of PFS ( $p < 0.001$ ). The radiomic score was an independent prognostic biomarker of survival in DLBCL patients. The extraction of RFs from baseline <sup>18</sup>F-FDG-PET might be proposed in DLBCL to stratify high-risk versus low-risk patients of relapse after first-line therapy, especially in low-IPI patients.

## KEYWORDS

DLCBL radiomics, PET lymphoma, PET radiomics, radiomic PET biomarker

Laura Lavinia Travaini and Francesca Botta first authors contributed equally. Sara Raimondi and Francesco Ceci last authors have co-senior authorship.

This is an open access article under the terms of the [Creative Commons Attribution-NonCommercial-NoDerivs](https://creativecommons.org/licenses/by-nc-nd/4.0/) License, which permits use and distribution in any medium, provided the original work is properly cited, the use is non-commercial and no modifications or adaptations are made.

© 2023 The Authors. Hematological Oncology published by John Wiley & Sons Ltd.

## 1 | INTRODUCTION

Diffuse large B-cell lymphoma (DLBCL) represents the most frequent non-Hodgkin's lymphoma subtype (30%–58% of all cases) with an incidence of 3.8/100 000/year in Europe.<sup>1</sup> Standard first-line therapy is based on the combination of the anti CD20 monoclonal antibody Rituximab with CHOP chemotherapy (R-CHOP regimen: Rituximab, cyclophosphamide, doxorubicin, vincristine, and prednisone). Based on a recent survey, the 5-year overall survival (OS) rate is 65%, indicating that 30%–40% of all patients will progress or relapse after primary treatment.<sup>2</sup> These high-risk patients may be partially identified by the current clinical prognostic scoring systems, such as the International Prognostic Index (IPI), which is based on 5 clinical variables (age, stage, performance status, number of extranodal sites, serum levels of lactate dehydrogenase).<sup>3</sup> In general, these models do not consider the biology of the disease, and for this reason still hold some limitations, especially in early stage disease, where treatment is often de-escalated.<sup>4</sup> Although in the last 20 years several studies identified biomarkers and gene expression profiling (GEP) based-signatures with prognostic potential, these progresses did not translate yet in improved prognostic stratification or in precision therapy strategies available in clinical practice. For example, GEP and genomic studies produced a series of prognostic models, such as the cell of origin classification<sup>5</sup> and algorithms based on complex integration of diverse molecular profiling studies.<sup>6,7</sup> However, most of these models are difficult to reproduce, technically challenging and applicable only in academic centers. Currently, the only biological parameter with clinical implication is the presence or absence of concurrent rearrangements of the MYC and BCL-2 and/or BCL-6 oncogenes, which defines a subset of high-grade B-cell lymphoma patients eligible for intensive chemoimmunotherapy regimens.<sup>8,9</sup> Current evidence suggests that MYC-positive tumors, presenting increased glucose metabolism, are characterized by metabolic heterogeneity.<sup>10,11</sup> DLBCL is a [<sup>18</sup>F]Fluorodeoxyglucose (FDG) avid neoplasm and [<sup>18</sup>F]FDG-Positron Emission Tomography ([<sup>18</sup>F]FDG-PET) is recommended for initial staging, assessment of response to therapy and re-staging in case of relapse clinically suspected.<sup>12</sup> Furthermore, through the assessment of metabolic tumor volume (MTV)<sup>13</sup> or Standardized Uptake Value (SUV) parameters<sup>14,15</sup> [<sup>18</sup>F]FDG-PET can be used as prognostic biomarker to identify those patients at worst prognosis.<sup>16</sup> Recently, radiomics, a novel high throughput quantitative analysis, gained interest allowing to characterize tumor biology and intra-tumor heterogeneity through the identification of quantitative imaging biomarkers named radiomic features (RFs).<sup>17–19</sup>

## 2 | MATERIALS AND METHODS

### 2.1 | Objectives

The primary objective of this analysis was to evaluate the association between the radiomic score, derived from the RFs extracted from

[<sup>18</sup>F]FDG-PET images, and progression free survival (PFS) and overall survival (OS), in DLBCL patients eligible for standard-of-care first line chemotherapy.

Secondary objectives were: a) to evaluate the association of standard [<sup>18</sup>F]FDG-PET metabolic parameters (SUV derivatives, MTV and TLG [total lesion glycolysis]) with PFS and OS; b) to compare the performance of the radiomic score with IPI and conventional PET-parameters model.

### 2.2 | Study design and patients selection

This is a retrospective, single-center, single-arm, open-label study on DLBCL patients treated and followed-up at our institution. Clinical records of patients from September 2008 to October 2019 (study cut-off date) were evaluated. Inclusion criteria were: (1) biopsy or histologically proven DLBCL; (2) [<sup>18</sup>F]FDG-PET as baseline procedure prior to first-line chemotherapy; (3) availability of all clinical, pathology and imaging data (no lost follow-up); (4) at least 24 months of follow-up. Exclusion criteria were: (1) [<sup>18</sup>F]FDG-PET performed outside our institution; (2) low quality PET images (e.g., wrong input of PET parameters, glycemia >200 mg/dl, para-vein injection, 2D scanners). The study was approved by the local ethical committee and institutional scientific review board (IEO Trial-ID: 2863).

### 2.3 | PET acquisition protocol

[<sup>18</sup>F]FDG-PET was performed with standard procedure according to the European guidelines.<sup>20</sup> PET images were acquired on DiscoveryST or Discovery600 PET/CT scanner (GE Healthcare, Waukesha, WI). Patients were injected with 3.3 (range 2.3–4.7) MBq/kg of [<sup>18</sup>F]FDG, and images were acquired 66 ± 11 min (median ± standard deviation SD) after injection, at 2.5 ± 0.5 min/bed. PET images were reconstructed with OSEM algorithm VUE point (2 iterations, 30 subset, 4.5 mm Gaussian post-filter) for DiscoveryST, and with OSEM algorithm VUE point HD (2 iterations, 16 subset, 5 mm Gaussian post-filter) for Discovery600. A low-dose CT scan was performed for attenuation correction of PET emission data and anatomical location.

### 2.4 | Image analysis and radiomic features extraction

Quantitative PET images analysis was performed with LifeX 6.32 package.<sup>21</sup> A pilot study was performed<sup>22</sup> comparing six different segmentation methods among those most widely used in the literature for lymphoma,<sup>23</sup> to select the most suitable method for the subsequent radiomic analysis. The main points of this study are summarized in the Supplementary Materials (Pilot study on Pet segmentation paragraph). Based on those results, an experienced nuclear medicine physician (LLT) drew a Region of Interest (ROI) for each lesion applying a SUV threshold equal to 25% of the maximum

SUV ( $SUV_{max}$ ) in the lesion (Figure 1). Total MTV (TMTV) was calculated summing all the lesions' volumes for each patient. Whole-body TLG (WTLG) was calculated as the sum of TLG values in each lesion. For each patient, radiomic analysis was performed on the target lesion, selected as the lesion with highest  $SUV_{max}$  (" $SUV_{max}$  lesion"). Fifty-three ( $n = 53$ ) RFs were calculated for each lesion; RFs list and description are reported in Supplementary Material Table S5, with the settings adopted for calculation [ $^{18}F$ ]FDG-PET quantitative data included in the main analysis were:  $SUV_{max}$ , TMTV, volume of the representative lesion (Vol ( $SUV_{max}$  lesion)), WTLG, and 53 RFs.

Image acquisition and clinical parameters which might affect PET image signal and texture (scanner model, frame duration, injected activity/body weight, time between injection and acquisition, glucose level) were collected to evaluate RFs reproducibility. After RFs log transformation, an ANOVA model was fitted for each RFs and parameter, to identify RFs affected by any parameter. RFs with False Discovery Rate (FDR)-adjusted  $p$ -values  $< 0.05$  were excluded by the analysis.

## 2.5 | Outcome measurements and statistical analysis

PFS was calculated from the date of diagnosis to the date of progression after first-line chemotherapy or death for any cause or last follow-up, while OS was calculated from the date of diagnosis to the date of death for any cause or last follow-up. PFS and OS were investigated using three statistical models, defined as clinical model, radiomic model and clinical-radiomic model. The clinical model included IPI and conventional not-radiomic PET imaging variables

( $SUV_{max}$ , TMTV, Vol [ $SUV_{max}$  lesion] and WTLG). The radiomic model included a radiomic score obtained considering only the reproducible RFs after ANOVA analysis. The radiomic score was obtained by a Cox-Elastic Net model regression with regularization parameters,  $\alpha$  and  $\lambda$ , chosen by means of a 10-folds cross-validation as the combination maximizing the C-index. The final Elastic Net model was fitted using the optimal values of  $\alpha$  and  $\lambda$ , providing—for each RF retained in the model—the corresponding coefficient  $\beta$  for the calculation of the radiomic score. Then, the radiomic score was calculated as a linear combination of the selected RFs weighted by the coefficients of the Elastic Net model on the original data as here detailed: indicating with  $\beta_1, \beta_2, \dots, \beta_p$  the Elastic Net coefficients for each of the  $p$  RFs in the model, and  $x_{i1}, x_{i2}, \dots, x_{ip}$  the observed values of the features for the  $i$ th patient, the radiomic score was calculated for each patient as follows: radiomic score $_i = \beta_1 x_{i1} + \beta_2 x_{i2} + \dots + \beta_p x_{ip}$ . The clinical-radiomic model merged the clinical variables and the radiomic score.

First, the univariate association of each variable included in the clinical-radiomic model with PFS and OS was evaluated by Log-Rank rank test, after dichotomizing the continuous variables using the median value, and IPI as low:  $\leq 2$  and high:  $> 2$ .

Then, clinical and clinical-radiomic models were calculated with multivariable proportional-hazard Cox models including only variables showing significance at univariate Cox analysis ( $p < 0.05$ ). The Cox univariate model obtained with the radiomic score as continuous variable was referred to as radiomic model.

PFS and OS were also explored stratifying the population by IPI (low vs. high). Univariate (Log-Rank) and multivariable proportional-hazard Cox models were performed in each sub-group to identify the risk of progression and death according to radiomic score only (univariate) and radiomic score together with the clinical variables

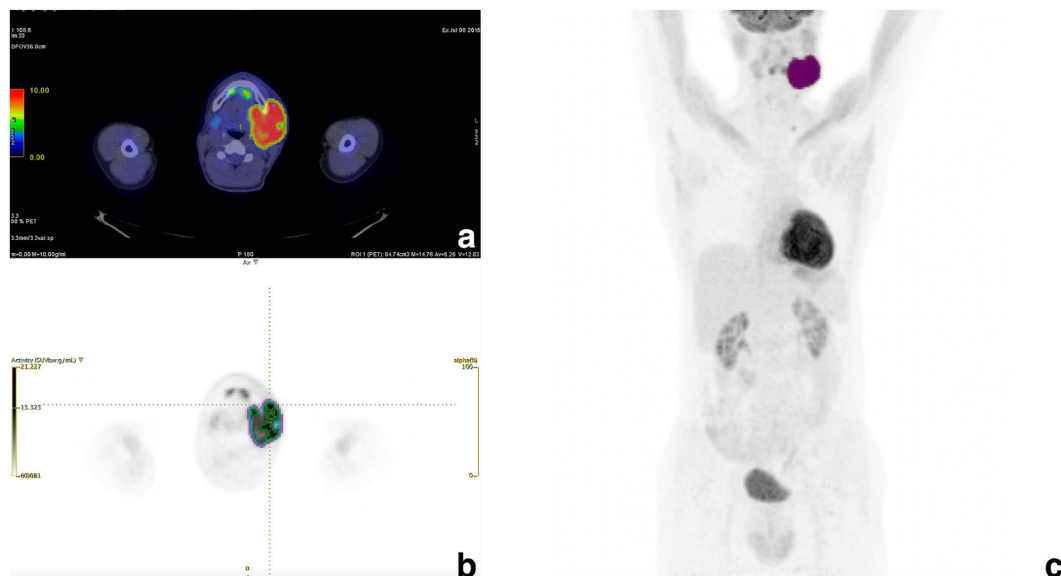


**FIGURE 1** Select axial slice (B) and maximum intensity projection (MIP) (C) from an FDG PET/CT study from a newly diagnosed DLBCL patient, prior to first-line chemotherapy, demonstrating three different contouring methods (pink = 25%  $SUV_{max}$ ; blue = 41%  $SUV_{max}$ ; green = 70%  $SUV_{max}$ ) performed with LifeX package. Select axial slice of fused [ $^{18}F$ ]-FDG PET/CT images with the contouring method (25%  $SUV_{max}$ ) superimposed (A).

used to define IPI: sex, age, serum LDH, number of extranodal site, stage (multivariable). The performances of the models were quantified and compared using the Harrell's C-index, with  $C = 1$  indicating optimal performance. 95% Confidence Intervals (CI) were obtained using the R package *survcomp*. Model evaluation by Harrell's C-index is recommended for survival analysis<sup>24,25</sup> and is commonly used for radiomic survival studies.<sup>26–28</sup> Statistical analysis was performed with R software, version 4.1.0.

### 3 | RESULTS

#### 3.1 | Patient population

One hundred and twelve patients ( $n = 112$ ) fulfilled the inclusion criteria (Figure 2). Population characteristics are summarized in Table 1. All patients were treated at our Institution with first-line R-CHOP/R-CHOP-like chemo immunotherapy and followed-up according to the best standard-of-care clinical practice. All 112 patients were evaluable for OS, and all but one ( $n = 111$ ) for PFS. In fact, for one patient we could not retrieve information on disease status at last follow-up, but only on OS status. Therefore, this patient was excluded from PFS analysis. The median follow-up was 34.7 months (Inter-Quartile Range (IQR) 11.3–66.3 months) for PFS and 41.1 (IQR 18.4–68.9) for OS. At the end of follow-up, 17% (19/112) relapsed and died with disease (median time to relapse 6.2 months): of these, 14 patients received second-line therapy and 5 received palliative/supportive care. One-year and 5-year survival rates were 83% and 73% for PFS, and 95% and 82% for OS.

#### 3.2 | Conventional parameters and radiomic analysis

Fifty-two ( $n = 52$ ) RFs were reproducible according to imaging and/or clinical parameters. Only one feature (GLCM\_2\_Correlation) was

TABLE 1 Baseline characteristics of study population.

Population characteristics ( $n = 112$ )	Median (IQR*)
Age at diagnosis (years)	62.3 (46.7–69.8)
Gender	$n$ (%)
Males	57 (51%)
Females	55 (49%)
Tumor stage	$n$ (%)
I	9 (8%)
II	31 (28%)
III	8 (7%)
IV	64 (57%)
IPI	$n$ (%)
0	9 (8%)
1	33 (29%)
2	28 (25%)
3	29 (26%)
4	12 (11%)
5	1 (1%)

Abbreviation: IQR, Interquartile range.

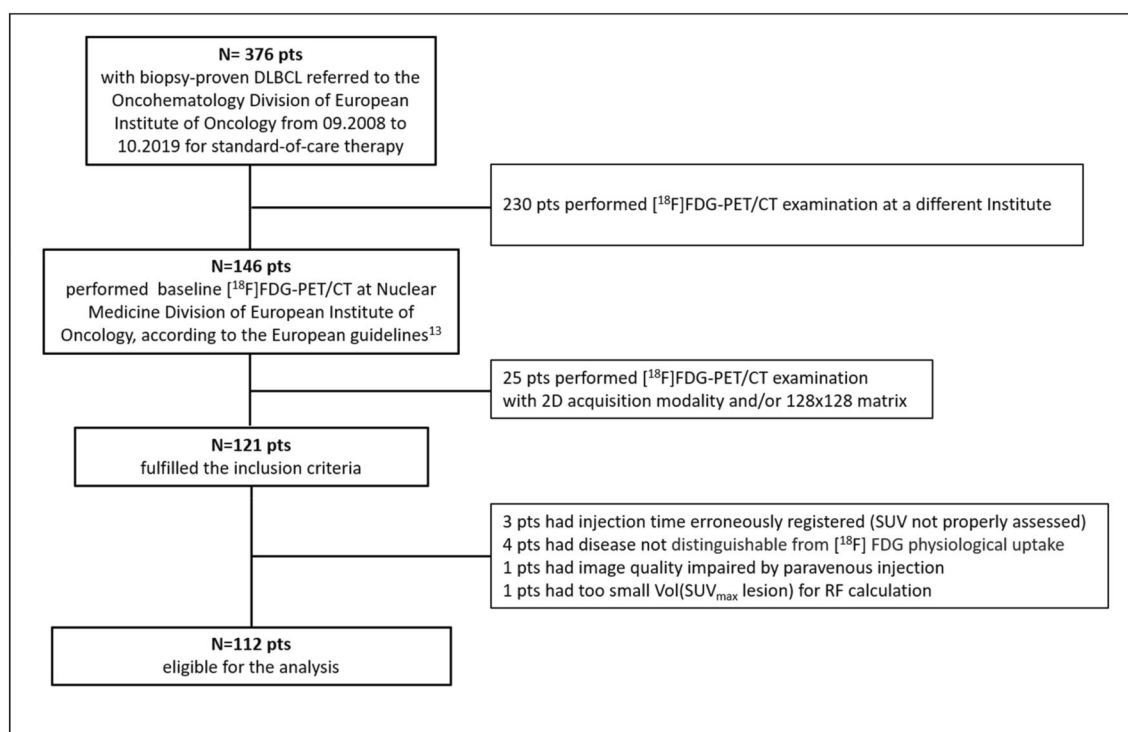


FIGURE 2 Patient selection flow chart.

non-reproducible at ANOVA due to significant dependence from scanner type, and was excluded from the analysis. The median (IQR) values of conventional PET imaging variables included in the clinical model were:  $SUV_{max}$  19.9 (11.3–26.0); TMTV 131.0 (45.2–371.8) ml; Vol ( $SUV_{max}$  lesion) 71.3 (19.8–219.7) ml; WTLG 1076.0 (264.9–3834.2)  $SUV \cdot ml$ .

Patients with high IPI (3–5) presented less favorable PFS and OS compared to patients with low IPI (0–2) at Log-Rank univariate analysis ( $p$ -values  $\leq 0.01$ , Figure S1). Demographic and clinical characteristics of the low/high IPI groups are reported in Supplementary materials Table S6. None among conventional PET variables ( $SUV_{max}$ , TMTV, Vol ( $SUV_{max}$  lesion), WTLG) was significantly associated with either PFS or OS at univariate Log-Rank test (all  $p > 0.05$ ).

The relevant features significantly associated with both PFS and OS were mainly texture features: NGLDM\_Coarseness, GLZLM\_Low Gray-level Zone Emphasis (LGZE), GLZLM\_Short-Zone Low Gray-level Emphasis (SZLGE), GLRLM\_Short-Run Low Gray-level Emphasis (SRLGE), GLCM\_1\_Energy, GLRLM\_Low Gray Level Run Emphasis (LGRE), GLZLM\_Short-Zone Emphasis (SZE), Sphericity, and HISTO\_Uniformity. The RFs selected by the model as mostly associated with PFS and OS were used to build the corresponding PFS and OS radiomic scores (Tables S7 and S8). Kaplan-Meier analysis yielded significant association of the dichotomized radiomic score (low = below median value; high = above median value) with PFS (Figure 3A) and OS (Figure 3B) (all  $p < 0.001$ ). Demographic and clinical characteristics of the low/high radiomic score groups are reported in Supplementary Material (Table S9 and S10).

### 3.3 | Clinical, radiomic and clinical-radiomic models

The associations of the variables included in the clinical model and radiomic score with PFS and OS (Cox models) are reported in Tables 2 and 3. IPI score (0–2 vs. 3–5), TMTV and the radiomic score were significantly associated with PFS and OS in univariate analysis. Only radiomic score and IPI score remained independent PFS and OS predictors in the multivariate models (all  $p < 0.01$ ). Clinical models' accuracy (C-index) was 0.68 for PFS and 0.78 for OS; C-index increased up to 0.81 (PFS) and 0.84 (OS) for radiomic models, and 0.83 for PFS and 0.90 for OS when considering the clinical-radiomic models. Stratifying the population according to IPI score (low-IPI vs. high-IPI), the radiomic score remained a significant independent predictor of PFS and OS (Figure 4). Demographic and clinical characteristics for the low versus high radiomic score patients within the low-IPI/high-IPI groups are reported in Supplementary Materials (Tables S11 for PFS and Table S12 for OS). The radiomic score confirmed its prognostic significance also after adjusting the model according to the clinical variables used to calculate IPI score (Tables S13 and S14). Specifically, patients with low radiomic score had a significantly more favorable PFS than patients with high radiomic score both in high-IPI group (Log-rank test  $p < 0.001$ , Figure 4A; multivariable Cox  $p = 0.004$ , Table S13) and in low-IPI group (Log-rank test  $p = 0.02$ , Figure 4C; multivariable Cox  $p = 0.02$ , Table S13).

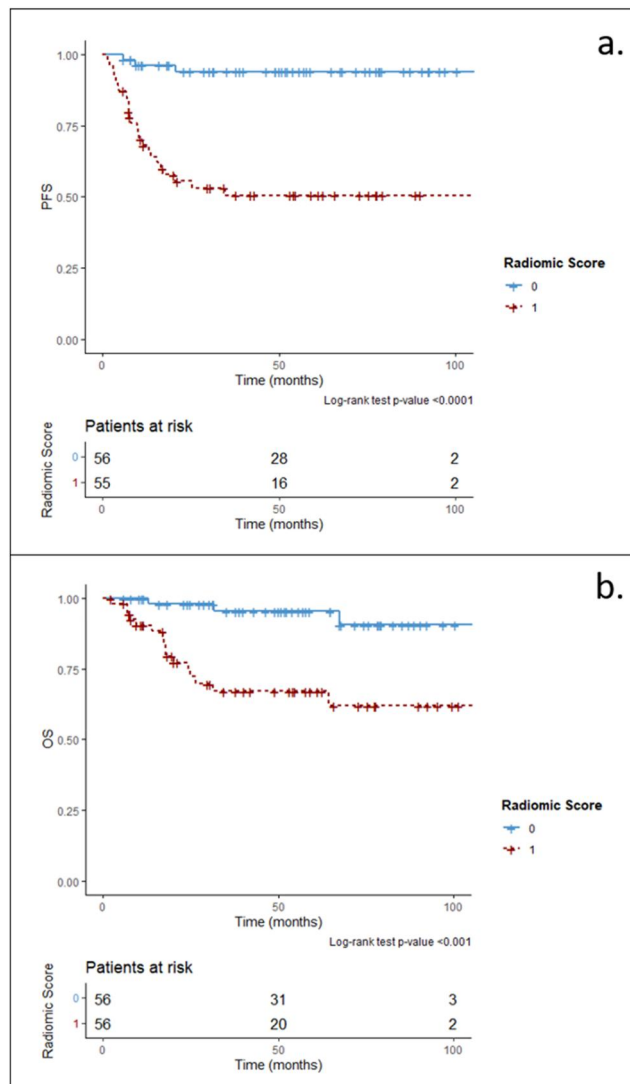


**FIGURE 3** Univariate association (Log-Rank rank test) between dichotomized radiomic score (0 = low; 1 = high) and (A) Progression Free Survival (PFS); (B) Overall Survival (OS).

Conversely, the radiomic score was an independent predictor of OS in high-IPI group (Log-rank test  $p < 0.001$ , Figure 4B; multivariable Cox  $p = 0.001$ , Table S14), while it was not associated with OS in low-IPI group (Log-rank test  $p = 0.49$ , Figure 4D; multivariable Cox  $p = 0.51$ , Table S14).

## 4 | DISCUSSION

In this study, the IPI score was a significant predictor of patients' outcome in univariate and multivariate analyses, as expected,<sup>3</sup> while the standard PET parameter TMTV showed a significant association with PFS and OS at univariate analysis only (Table 2 and Table 3). The other PET conventional parameters ( $SUV_{max}$ , WTLG and the volume of the highest uptake lesion) were not associated with PFS or OS in our population. These results are partially in contrast with those reported previously. Other studies,<sup>14–16,29</sup> reported the role for PET

**TABLE 2** Univariate and multivariable Hazard Ratio (HR) with 95% Confidence Intervals (CI) for the association of continuous clinical variables and radiomic score with progression free survival.

Variable	Univariate		Multivariable (clinical)		Multivariable (clinical-radiomic)		
	HR (95% CI)	p-value	HR (95% CI)	p-value	HR (95% CI)	p-value	
SUV <sub>max</sub>	0.98 (0.94–1.01)	0.15	-	-	-	-	
TMTV*	<b>1.07 (1.01–1.13)</b>	<b>0.02</b>	1.04 (0.98–1.10)	0.16	0.99 (0.93–1.05)	0.66	
Vol(SUV <sub>max</sub> lesion)*	1.04 (0.98–1.10)	0.17	-	-	-	-	
WTLG**	1.02 (0.96–1.07)	0.55	-	-	-	-	
IPI	Low	1.00 (Ref)	-	-	1.00 (Ref)	-	
	High	<b>2.60 (1.25–5.48)</b>	<b>0.01</b>	<b>2.23 (1.02–4.91)</b>	<b>0.05</b>	<b>2.68 (1.22–5.86)</b>	<b>0.01</b>
Radiomic score	<b>3.56 (2.29–5.54)</b>	<b>&lt;0.0001</b>	-	-	<b>3.65 (2.26–5.89)</b>	<b>&lt;0.0001</b>	

Note: Statistically significant variables are reported in bold.

\*100 units increase (from mL to dL).

\*\*1000 units increase (from SUV\*mL to SUV\*L).

**TABLE 3** Univariate and multivariable Hazard Ratio with 95% Confidence Intervals (CI) for the association of clinical variables and radiomic score with overall survival.

Variable	Univariate		Multivariable (clinical)		Multivariable (clinical-radiomic)		
	HR (95% CI)	p-value	HR (95% CI)	p-value	HR (95% CI)	p-value	
SUV <sub>max</sub>	1.00 (0.96–1.04)	0.92	-	-	-	-	
TMTV*	<b>1.09 (1.03–1.16)</b>	<b>0.02</b>	1.04 (0.97–1.11)	0.24	0.98 (0.92–1.05)	0.54	
Vol(SUV <sub>max</sub> lesion)*	1.06 (0.99–1.12)	0.10	-	-	-	-	
WTLG**	1.04 (0.99–1.10)	0.11	-	-	-	-	
IPI	Low	1.00 (Ref)	-	-	1.00 (Ref)	-	
	High	<b>10.20 (2.97–35.01)</b>	<b>0.0002</b>	<b>8.83 (2.49–31.37)</b>	<b>0.0008</b>	<b>8.12 (2.25–29.36)</b>	<b>0.001</b>
Radiomic score	<b>3.83 (2.37–6.20)</b>	<b>&lt;0.0001</b>	-	-	<b>3.08 (1.94–4.88)</b>	<b>&lt;0.0001</b>	

Note: Statistically significant variables are reported in bold.

\*100 units increase (from mL to dL).

\*\*1000 units increase (from SUV\*mL to SUV\*L).

standard parameters as predictors of patient survival, in some cases outperforming IPI.<sup>15,30,31</sup> These discordant results might be related to the heterogenous populations enrolled, discrepancies in follow-up lengths, and to the different methodologies applied to extract PET parameters.

The radiomic score was an independent predictor of PFS and OS, alone and in association with IPI score (Figure 3, Table 2 and Table 3). Second-order features (quantifying different properties of image texture) were the main contributors for PFS and OS prediction. Notably, most RFs were associated with both endpoints. This result suggests the robustness of the RFs included in the radiomic score, supporting the hypothesis that relevant and novel prognostic information can be obtained by RFs. The most relevant features (*Coarseness* from Neighboring Gray Level Dependence Matrix, *Low Gray-level Zone Emphasis* [LGZE] and *Short-Zone Low Gray-level Emphasis* [SZLGE] from Gray Level Zone Length Matrix and *Short-Run Low Gray-level Emphasis* [SRLGE] from Gray Level Run Length Matrix) were related to the presence and distribution of low intensity zones,

in particular small zones with homogeneous low uptake, and to the distribution of short runs (consecutive voxels along a defined direction) with homogeneous low uptake. Interestingly, the RFs associated with outcomes in our series were previously shown to be representative of a heterogeneous microenvironment (i.e., hypoxia and necrosis) where malignant clones, extracellular microenvironment and fibroblast coexist.<sup>32,33</sup> Parvez et al<sup>17</sup> described a prognostic role of RFs derived by Gray Level Zone Length Matrix associated with Disease Free Survival, while Aide et al<sup>34</sup> observed the association of these RFs with the 2-year event-free survival, and Kun-Han-Lue et al<sup>35</sup> found a significant association of RFs extracted from Gray Level Run Length Matrix with both PFS and OS. Accordingly, our results confirmed the hypothesis that novel prognostic biomarkers derived by quantitative analysis of PET image, combined with clinical parameters, might be reliable predictors of survival.

The identification of low-IPI patients at higher risk of relapse after primary therapy could be clinically relevant, given that current treatment guidelines recommend therapy de-escalation in early stage

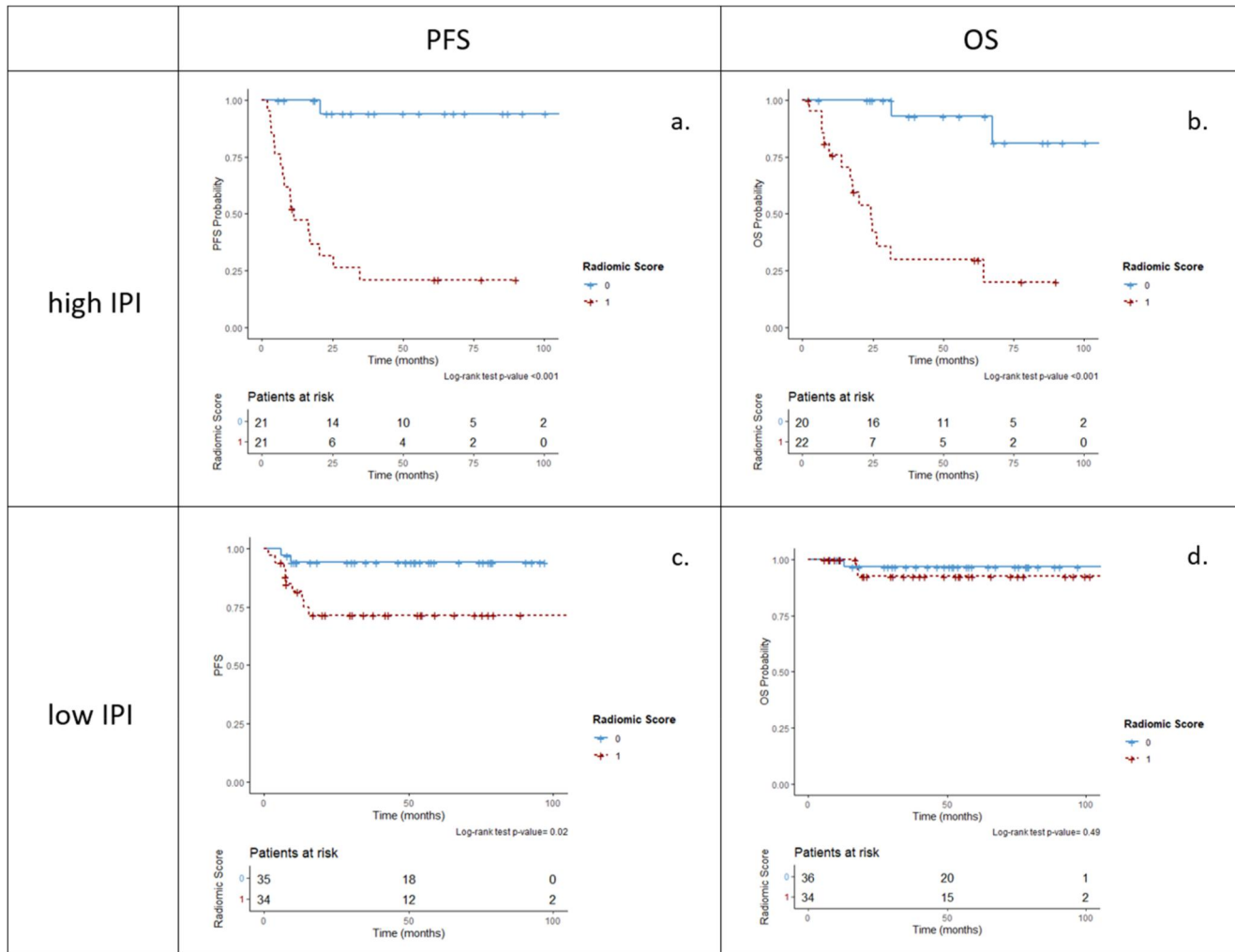


**FIGURE 4** Survival curves for Progression-Free Survival (PFS) and Overall Survival (OS) according to radiomic score (0 = low; 1 = high) for patients with (A-B) IPI = High and (C-D) IPI = Low.

DLBCL.<sup>36</sup> Interestingly, in the low-IPI subgroup demographic and clinical characteristics were comparable in patients with high versus low PFS radiomic score (Supplementary Table S11). Considering the high-IPI patients, the association of the radiomic score with both PFS and OS was strong (Figures 4A,B; Supplementary Table S13 and S14). However, in this sub-cohort, a significant age difference was observed between patients with low versus high radiomic score (mean age 60.1 vs. 70.9 years for PFS, 61.4 vs. 69.2 for OS, Supplementary Table vS11 and S12). This result suggests the potential role of age as confounding factor since older patients are generally characterized by a poor outcome compared to the younger ones.<sup>37</sup> However, in our cohort the outcome of patients with low radiomic score was extremely favorable regardless the IPI score. These findings may suggest that the radiomic might be a reliable tool to identify a biologically distinct DLBCL subset characterized by enhanced sensitivity to standard chemoimmunotherapy.

This study is not exempt from limitations. First, the retrospective design of the study might have affected patient selection. Second, the small sample size did not allow the separation between training and

validation set. In case of small cohorts, indeed, this approach is not recommended.<sup>38</sup> However, we applied an internal repeated k-fold cross validation to reduce the probability of overfitting. Nevertheless, before applying our model to the clinical setting, external validation is needed.

On the other side, strengths are represented by the long follow-up available (median 34.7 months, IQR 11.3–66.3 months), the treatment scheme homogeneity (selected following international guidelines), and a robust methodology for PET images analysis. The latter included the choice of single Institute images with comparable PET scanners, and ANOVA reproducibility analysis to avoid the influence of acquisition and reconstruction settings on RFs.<sup>39</sup> Notably, ANOVA did not identify significant influence, probably due to imaging procedure standardization in our center. In addition, to test and support the robustness of the methodology, a preliminary analysis was performed to select the most reliable PET segmentation method, including a sensitivity analysis to assess the differences in model performance when changing segmentation method or when considering different target lesions.<sup>22</sup> Since no significant difference was



found among the tested methodologies, the results obtained with only one segmentation method and target lesion were included in this study. The generalizability of the models needs to be confirmed with external validation on independent populations, also with the inclusion of novel parameters appearing promising for their prognostic role in recent studies.<sup>18,19,40</sup>

## 5 | CONCLUSION

The radiomic score outperformed conventional PET parameters as independent predictor of survival in patients affected by DLCL who performed baseline [<sup>18</sup>F]FDG-PET prior to first-line therapy. Furthermore, the development of a clinical-radiomic model, integrating clinical parameters and the radiomic score, demonstrated the highest prognostic accuracy among different models analyzed. While far from being considered a replacement of the IPI score, the radiomic score might be proposed as baseline prognostic biomarker to refine risk stratification in DLCL. Additional data obtained in a multicentre setting are needed to confirm this hypothesis and to externally validate the models.

## ACKNOWLEDGMENTS

None.

Open access funding provided by BIBLIOSAN

## CONFLICT OF INTEREST STATEMENT

All the authors declare that they have no potential conflict of interest related to this study.

## DATA AVAILABILITY STATEMENT

The data that support the findings of this study are available on request from the corresponding author. The data are not publicly available due to privacy or ethical restrictions.

## ETHICS STATEMENT

All procedures performed in studies involving human participants were in accordance with the ethical standards of the institutional and/or national research committee and with the 1964 Helsinki Declaration and its later amendments or comparable ethical standards. The study was approved by the local ethical committee and institutional scientific review board (IEO Trial-ID: 2863).

## ORCID

Laura Lavinia Travaini  <https://orcid.org/0000-0002-8084-5649>

Enrico Derenzini  <https://orcid.org/0000-0002-7154-8140>

Lighea Simona Airò Farulla  <https://orcid.org/0000-0003-3540-258X>

## PEER REVIEW

The peer review history for this article is available at <https://www.webofscience.com/api/gateway/wos/peer-review/10.1002/hon.3171>.

## REFERENCES

1. Sant M, Allemani C, Tereanu C, et al. Incidence of hematologic malignancies in Europe by morphologic subtype: results of the HAE-MACARE project. *Blood*. 2010;116(19):3724-3734. <https://doi.org/10.1182/blood-2010-05-282632>
2. Harrysson S, Eloranta S, Ekberg S, et al. Incidence of relapsed/refractory diffuse large B-cell lymphoma (DLBCL) including CNS relapse in a population-based cohort of 4243 patients in Sweden. *Blood Cancer J*. 2021;11(1):9. <https://doi.org/10.1038/s41408-020-00403-1>
3. International Non-Hodgkin's Lymphoma Prognostic Factors Project (1993). A predictive model for aggressive non-Hodgkin's lymphoma. *N Engl J Med*. 329(14), 987-994. <https://doi.org/10.1056/NEJM199309303291402>
4. Poeschel V, Held G, Ziepert M, et al. Four versus six cycles of CHOP chemotherapy in combination with six applications of rituximab in patients with aggressive B-cell lymphoma with favourable prognosis (FLYER): a randomised, phase 3, non-inferiority trial. *Lancet (London, Engl)*. 2019;394(10216):2271-2281. [https://doi.org/10.1016/S0140-6736\(19\)33008-9](https://doi.org/10.1016/S0140-6736(19)33008-9)
5. Alizadeh AA, Eisen MB, Davis RE, et al. Distinct types of diffuse large B-cell lymphoma identified by gene expression profiling. *Nature*. 2000;403(6769):503-511. <https://doi.org/10.1038/35000501>
6. Chapuy B, Stewart C, Dunford AJ, et al. Molecular subtypes of diffuse large B cell lymphoma are associated with distinct pathogenic mechanisms and outcomes. *Nat Med*. 2018;24(5):679-690. <https://doi.org/10.1038/s41591-018-0016-8>
7. Reddy A, Zhang J, Davis NS, et al. Genetic and functional drivers of diffuse large B cell lymphoma. *Cell*. 2017;171(2):481-494. <https://doi.org/10.1016/j.cell.2017.09.027>
8. Green TM, Young KH, Visco C, et al. Immunohistochemical double-hit score is a strong predictor of outcome in patients with diffuse large B-cell lymphoma treated with rituximab plus cyclophosphamide, doxorubicin, vincristine, and prednisone. *J Am Soc Clin Oncol*. 2012;30(28):3460-3467. <https://doi.org/10.1200/JCO.2011.41.4342>
9. Johnson NA, Slack GW, Savage KJ, et al. Concurrent expression of MYC and BCL2 in diffuse large B-cell lymphoma treated with rituximab plus cyclophosphamide, doxorubicin, vincristine, and prednisone. *J Am Soc Clin Oncol*. 2012;30(28):3452-3459. <https://doi.org/10.1200/JCO.2011.41.0985>
10. Zhang J, Grubor V, Love CL, et al. Genetic heterogeneity of diffuse large B-cell lymphoma. *Proc Natl Acad Sci U S A*. 2013;110(4):1398-1403. <https://doi.org/10.1073/pnas.1205299110>
11. Voltin CA, Mettler J, Grosse J, et al. FDG-PET imaging for hodgkin and diffuse large B-cell lymphoma-an updated overview. *Cancers*. 2020;12(3):601. <https://doi.org/10.3390/cancers12030601>
12. Barrington SF, Mikhaeel NG, Kostakoglu L, et al. Role of imaging in the staging and response assessment of lymphoma: consensus of the international conference on malignant lymphomas imaging working group. *J Clin Oncol official*. 2014;32(27):3048-3058. <https://doi.org/10.1200/JCO.2013.53.5229>
13. Mikhaeel NG, Smith D, Dunn JT, et al. Combination of baseline metabolic tumour volume and early response on PET/CT improves progression-free survival prediction in DLBCL. *Eur J Nucl Med Mol Imag*. 2016;43(7):1209-1219. <https://doi.org/10.1007/s00259-016-3315-7>
14. Ceriani L, Martelli M, Zinzani PL, et al. Utility of baseline 18FDG-PET/CT functional parameters in defining prognosis of primary mediastinal (thymic) large B-cell lymphoma. *Blood*. 2015;126(8):950-956. <https://doi.org/10.1182/blood-2014-12-616474>
15. Kim TM, Paeng JC, Chun IK, et al. Total lesion glycolysis in positron emission tomography is a better predictor of outcome than the International Prognostic Index for patients with diffuse large B cell lymphoma. *Cancer*. 2013;119(6):1195-1202. <https://doi.org/10.1002/cncr.27855>

16. Cottreau AS, Lanic H, Mareschal S, et al. Molecular profile and FDG-PET/CT total metabolic tumor volume improve risk classification at diagnosis for patients with diffuse large B-cell lymphoma. *J Am Assoc Cancer Res*. 2016;22(15):3801-3809. <https://doi.org/10.1158/1078-0432.CCR-15-2825>
17. Parvez A, Tau N, Hussey D, Maganti M, Metser U. <sup>18</sup>F-FDG PET/CT metabolic tumor parameters and radiomics features in aggressive non-Hodgkin's lymphoma as predictors of treatment outcome and survival. *Ann Nucl Med*. 2018;32(6):410-416. <https://doi.org/10.1007/s12149-018-1260-1>
18. Eertink JJ, van de Brug T, Wiegers SE, et al. <sup>18</sup>F-FDG PET baseline radiomics features improve the prediction of treatment outcome in diffuse large B-cell lymphoma. *Eur J Nucl Med Mol Imag*. 2022;49(3):932-942. <https://doi.org/10.1007/s00259-021-05480-3>
19. Cottreau AS, Nioche C, Dirand AS, et al. <sup>18</sup>F-FDG PET dissemination features in diffuse large B-cell lymphoma are predictive of outcome. *J Nucl Med official Publ Soc Nucl Med*. 2020;61(1):40-45. <https://doi.org/10.2967/jnumed.119.229450>
20. Boellaard R, Delgado-Bolton R, Oyen WJ, et al. FDG PET/CT: EANM procedure guidelines for tumour imaging: version 2.0. *Eur J Nucl Med Mol Imag*. 2015;42(2):328-354. <https://doi.org/10.1007/s00259-014-2961-x>
21. Nioche C, Orhac F, Boughdad S, et al. LIFEx: a freeware for radiomic feature calculation in multimodality imaging to accelerate advances in the characterization of tumor heterogeneity. *Cancer Res*. 2018;78(16):4786-4789. <https://doi.org/10.1158/0008-5472.CAN-18-0125>
22. Botta F, Ferrari M, Raimondi S, et al. The impact of segmentation method and target lesion selection on radiomic analysis of <sup>18</sup>F-FDG PET images in diffuse large B-cell lymphoma. *Appl Sci*. 2022;12(19):9678. <https://doi.org/10.3390/app12199678>
23. Barrington SF, Meignan M. Time to prepare for risk adaptation in lymphoma by standardizing measurement of metabolic tumor burden. *J Nucl Med official Publ. Soc Nucl Med*. 2019;60(8):1096-1102. <https://doi.org/10.2967/jnumed.119.227249>
24. Harrel FE, Jr, Lee KL, Mark DB. Tutorial in biostatistics: multivariable prognostic models: issues in developing models, evaluating assumptions and adequacy, and measuring and reducing errors. *Statistics Med*. 1996;15(4):361-387. [https://doi.org/10.1002/\(sici\)1097-0258\(19960229\)15:4<361::aid-sim168>3.0.co;2-4](https://doi.org/10.1002/(sici)1097-0258(19960229)15:4<361::aid-sim168>3.0.co;2-4)
25. Pencina MJ, D'Agostino RB. Overall C as a measure of discrimination in survival analysis: model specific population value and confidence interval estimation. *Statistics Med*. 2004;23(13):2109-2123. <https://doi.org/10.1002/sim.1802>
26. Jiang C, Li A, Teng Y, et al. Optimal PET-based radiomic signature construction based on the cross-combination method for predicting the survival of patients with diffuse large B-cell lymphoma. *Eur J Nucl Med Mol Imag*. 2022;49(8):2902-2916. <https://doi.org/10.1007/s00259-022-05717-9>
27. Wang H, Zhao S, Li L, Rong T. Development and validation of an <sup>18</sup>F-FDG PET radiomic model for prognosis prediction in patients with nasal-type extranodal natural killer/T cell lymphoma. *Eur Radiol*. 2020;30(10):5578-5587. <https://doi.org/10.1007/s00330-020-06943-1>
28. Xu H, Abdallah N, Marion J-M, et al. Radiomics prognostic analysis of PET/CT images in a multicenter head and neck cancer cohort: investigating ComBat strategies, sub-volume characterization, and automatic segmentation. *Eur J Nucl Med Mol Imag*. 2023;50(6):1720-1734. <https://doi.org/10.1007/s00259-023-06118-2>
29. Xie M, Zhai W, Cheng S, Zhang H, Xie Y, He W. Predictive value of <sup>18</sup>F-FDG PET/CT quantization parameters for progression-free survival in patients with diffuse large B-cell lymphoma. *Hematology (N Y)*. 2016;21(2):99-105. <https://doi.org/10.1179/1607845415Y.0000000033>
30. Sasanelli M, Meignan M, Haioun C, et al. Pretherapy metabolic tumour volume is an independent predictor of outcome in patients with diffuse large B-cell lymphoma. *Eur J Nucl Med Mol Imag*. 2014;41(11):2017-2022. <https://doi.org/10.1007/s00259-014-2822-7>
31. Zhou M, Chen Y, Huang H, Zhou X, Liu J, Huang G. Prognostic value of total lesion glycolysis of baseline <sup>18</sup>F-fluorodeoxyglucose positron emission tomography/computed tomography in diffuse large B-cell lymphoma. *Oncotarget*. 2016;7(50):83544-83553. <https://doi.org/10.18632/oncotarget.13180>
32. Jin X, Wei M, Wang S, et al. Detecting fibroblast activation proteins in lymphoma using <sup>68</sup>Ga-FAPI PET/CT. *J Nucl Med official Publ Soc Nucl Med*. 2022;63(2):212-217. <https://doi.org/10.2967/jnumed.121.262134>
33. Staudt LM, Dave S. The biology of human lymphoid malignancies revealed by gene expression profiling. *Adv Immunol*. 2005;87:163-208. [https://doi.org/10.1016/S0065-2776\(05\)87005-1](https://doi.org/10.1016/S0065-2776(05)87005-1)
34. Aide N, Fruchart C, Nganoa C, Gac AC, Lasnon C. Baseline <sup>18</sup>F-FDG PET radiomic features as predictors of 2-year event-free survival in diffuse large B cell lymphomas treated with immunochemotherapy. *Eur Radiol*. 2020;30(8):4623-4632. <https://doi.org/10.1007/s00330-020-06815-8>
35. Lue KH, Wu YF, Lin HH, et al. Prognostic value of baseline radiomic features of <sup>18</sup>F-FDG PET in patients with diffuse large B-cell lymphoma. *Diagnostics*. 2020;11(1):36. <https://doi.org/10.3390/diagnostics11010036>
36. Tilly H, Gomes da Silva M, Vitolo U, et al. Diffuse large B-cell lymphoma (DLBCL): ESMO Clinical Practice Guidelines for diagnosis, treatment and follow-up. *Ann Oncol official J Eur Soc Med Oncol*. 2015;26(Suppl 5):v116-v125. <https://doi.org/10.1093/annonc/mdv304>
37. Cancer Stat Facts: NHL – Diffuse Large B-Cell Lymphoma (DLBCL) [Internet]. 2018 [cited 2022 Apr 21]. <https://seer.cancer.gov/statfacts/html/dlbcl.html>
38. Steyerberg EW. Validation in prediction research: the waste by data splitting. *J Clin Epidemiol*. 2018;103:131-133. <https://doi.org/10.1016/j.jclinepi.2018.07.010>
39. Zwanenburg A. Radiomics in nuclear medicine: robustness, reproducibility, standardization, and how to avoid data analysis traps and replication crisis. *Eur J Nucl Med Mol Imag*. 2019;46(13):2638-2655. <https://doi.org/10.1007/s00259-019-04391-8>
40. Eertink J, Zwezerijnen G, Cysouw M, et al. Comparing lesion and feature selections to predict progression in newly diagnosed DLBCL patients with FDG PET/CT radiomics features. *Eur J Nucl Med Mol Imag*. 2022;49(13):4642-4651. <https://doi.org/10.1007/s00259-022-05916-4>

## SUPPORTING INFORMATION

Additional supporting information can be found online in the Supporting Information section at the end of this article.

**How to cite this article:** Travaini LL, Botta F, Derenzini E, et al. [<sup>18</sup>F]-FDG PET radiomic model as prognostic biomarker in diffuse large B-cell lymphoma. *Hematol Oncol*. 2023;1-9. <https://doi.org/10.1002/hon.3171>